ELECTRON INELASTIC MEAN FREE PATHS IN SOLIDS AT LOW ENERGIES

S. TANUMA,[1] C.J. POWELL[2] and D.R. PENN[2]

[1]Central Research Laboratories, Nippon Mining Company Ltd., 3-17-35 Niizo-Minami, Toda, Saitama 335, Japan

[2]National Institute of Standards and Technology, Gaithersburg, MD 20899, USA

ABSTRACT

We have calculated electron inelastic mean free paths (IMFPs) for 50-200 eV electrons in 31 materials (27 elements and 4 compounds). These calculations extend those previously reported for 200-2000 eV electrons in the same materials but avoid an approximation valid for electron energies above 200 eV. IMFP results are presented in this paper for magnesium, aluminum, silicon, nickel, copper, and gold. The IMFP dependence on electron energy in the range 50-200 eV varies considerably from material to material; these variations are associated with substantial differences in the electron energy-loss functions amongst the materials. We have also extended the general IMFP formula derived earlier to describe the calculated IMFPs over the 50-2000 eV energy range.

INTRODUCTION

Values of inelastic mean free paths (IMFPs) and attenuation lengths (ALs) are needed in quantitative surface analysis by Auger-electron spectroscopy (AES) and x-ray photoelectron spectroscopy (XPS) as well as for determining the surface sensitivity of other electron spectroscopies. The terms IMFP, AL, and escape depth are often used interchangeably but each has a separate meaning (1,2). The IMFP can be obtained from theory and certain types of experiments, while the AL is obtained from overlayer-film experiments and with use of a model in which the effects of elastic electron scattering are ignored. The escape depth is the product of the AL and the cosine of the angle defined by the analyzer direction and the surface normal (e.g., in an AES or XPS experiment). The IMFP is systematically larger than the AL by up to about 35% (3).

We have previously reported (4) new calculations of IMFPs for 200-2000 eV electrons in 27 elements (C, Mg, Al, Si, Ti, V, Cr, Fe, Ni, Cu, Y, Zr, Nb, Mo, Ru, Rh, Pd, Ag, Hf, Ta, W, Re, Os, Ir, Pt, Au, and Bi) and 4 compounds (LiF, SiO_2, ZnS, and Al_2O_3). We fitted our calculated IMFPs to the Bethe equation for inelastic electron scattering and were able to obtain empirical expressions for the two Bethe parameters in terms of several material constants. The resulting general IMFP formula could then be used to predict IMFPs in other materials.

Our IMFP calculations have now been extended to lower energies (50 eV). We present here some of the new IMFP results and point out substantial differences in the energy dependences of the IMFPs in the 50-200 eV range. These differences are substantially greater than expected from a simple AL formula (5) that is in widespread use. We have also modified our previous general IMFP formula so that it can be applied over the 50-2000 eV energy range.

PROCEDURE

Our IMFP calculations are based on an algorithm developed by Penn (6) which should be applicable to a wide range of materials. Experimental optical data are used to give information on the inelastic scattering probability as a function of energy loss for each material and theory is used to describe the dependence of the scattering probability on momentum transfer. This hybrid approach enables us to take advantage of available optical data which has been checked for internal consistency with two sum rules (4). We are particularly interested in using the algorithm in a consistent way to determine IMFP dependences on material and electron energy since AL measurements are extremely difficult to perform with the needed accuracy (1,7).

The IMFPs are calculated from Eqs. (1) and (14) given in our previous paper (4). The IMFP values reported in that paper were obtained with an approximation valid above 200 eV. The Penn algorithm neglects vertex corrections, self-consistency, and the effects of exchange and correlation; the results are therefore expected to be useful for energies above about 50 eV.

IMFP calculations were made for the same 27 elements and 4 compounds we examined previously (4); these materials were selected because suitable optical data were conveniently available. The methods by which the optical data were checked have been reported (4). Values of the energy-loss function $\mathrm{Im}[-1/\epsilon(\Delta E)]$ were calculated from the complex dielectric constant $\epsilon(\Delta E)$ as a function of electron energy loss ΔE (or photon energy).

All energies are reported here with reference to the Fermi level. A parameter in the IMFP calculation is the Fermi energy (or width of the conduction band); these values have been taken from band-structure calculations for the elemental solids (8). It was found that the calculated IMFPs were not sensitive to this parameter and so estimates from free-electron theory were made for the four compounds.

RESULTS AND DISCUSSION

Figures 1 and 2 show calculated IMFPs at energies below 200 eV for six representative solids: Mg, Al, Si, Ni, Cu, and Au; results for the other materials will be reported elsewhere (9). Although the IMFP values at energies

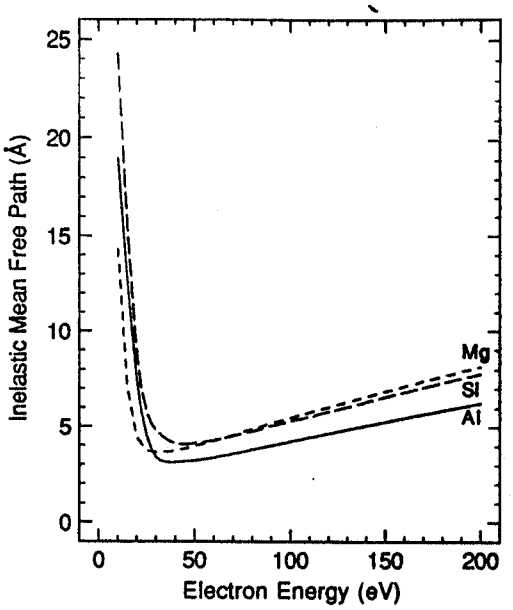

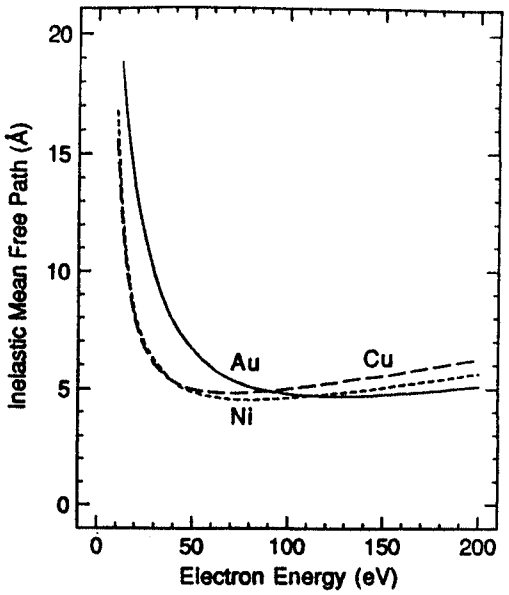

Fig. 1. Plots of the calculated IMFPs for Mg (short-dashed line), Al (solid line), and Si (long-dashed line) as a function of electron energy.

Fig. 2. Plots of the calculated IMFPs for Ni (short-dashed line), Cu (long-dashed line), and Au (solid line).

below 50 eV may not be reliable, we present these results to show the IMFP dependence on energy in the vicinity of the minima. The IMFPs for Mg, Al, and Si show minima at energies of about 30-40 eV (Fig. 1) while the IMFP calculations for Ni, Cu, and Au show minima at about 70-140 eV (Fig. 2).

The results of Figs. 1 and 2 are not surprising since Mg, Al, and Si are free-electron-like solids. For such materials, the dominant inelastic scattering mechanism in the bulk is volume-plasmon excitation (10). The volume plasmon energies for these solids are about 10 eV, 15 eV, and 17 eV, respectively, and it would be expected that the maximum inelastic scattering cross sections (and the minimum IMFPs) would occur for electron energies several times the principal excitation energies (11).

By contrast, the inelastic electron scattering in transition and noble metals is largely due to single-electron excitations (10). The energy-loss functions for these solids consist of broad, overlapping structures in the 10-80 eV range. The structures associated with valence-electron and core-electron excitations also overlap to an extent that it is not possible to make meaningful distinctions among them (10). The broad minima in Fig. 2 for Ni, Cu, and Au are thus consistent with the broad energy-loss spectra for these metals and, possibly, more complex dependences of the excitation cross sections for the various inelastic channels on electron energy (11).

It is useful to analyze the computed IMFPs in terms of the Bethe equation for inelastic electron scattering (12). This equation can be written in the form (4):

$$\lambda = E/[E_p^2 \beta \ln(\gamma E)] \quad \text{Å} \qquad [1]$$

where λ is the IMFP as a function of electron energy E (in eV), $E_p = 28.8 (N_v \rho/A)^{1/2}$ is the free-electron plasmon energy (in eV), ρ is the bulk density (in g/cm^3), A is the atomic or molecular weight, and N_v is the number of valence electrons per atom or molecule. The parameter $\beta = M_{tot}^2/28.8\ N_v$ where M_{tot}^2 is the square of the dipole matrix element for all available inelastic scattering processes and can be computed from an integral of the energy-loss function (4). The parameter γ is a complicated function of the dependence of the energy-loss function on momentum transfer.

Since the Bethe equation is expected to be valid if the electron energy is sufficiently high, this equation provides a useful means of analyzing calculated or measured IMFPs (13) or cross sections (14). The analysis is performed simply by constructing a Fano plot (15) in which values of E/λ are plotted versus $\ln E$. If such a plot is linear and the slope is as expected from established optical data (i.e., the value of M_{tot}^2), the set of data is consistent with Eq. [1] and the optical data. The Fano plots typically have

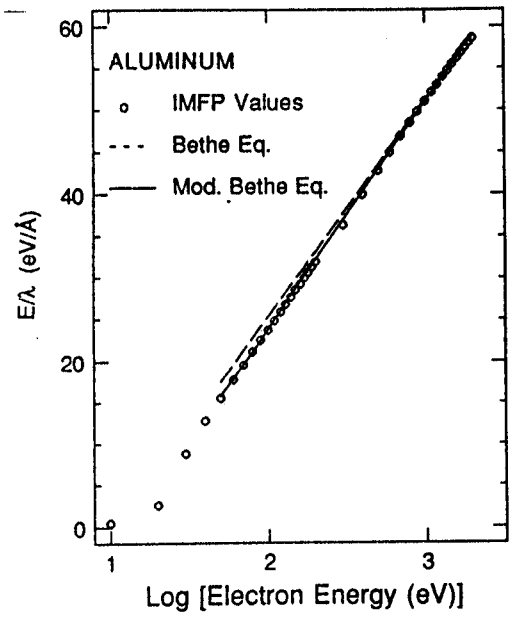

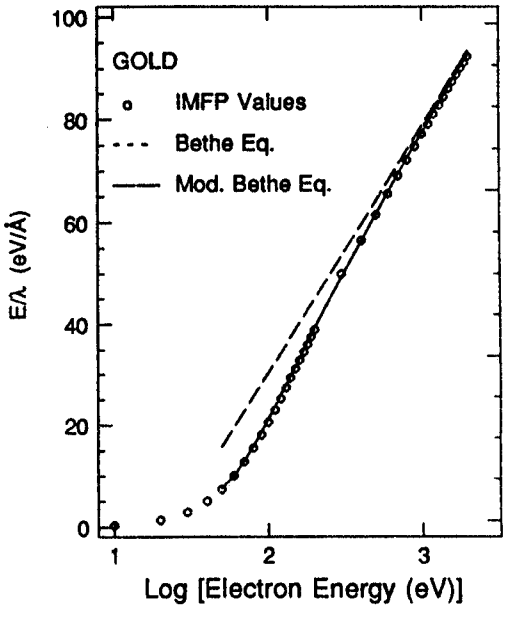

Fig. 3. Fano plot for aluminum. The open circles show the calculated IMFP values, the solid line a fit with Eq. [2], and the dashed line the first term of Eq. [2] (i.e., the Bethe equation).

Fig. 4. Fano plot for gold. See caption to Fig. 3.

two linear regions, however, and it is only for the linear region at higher energies that consistency with optical data is attained (11,16). The Fano plot is thus convenient for determining the minimum electron energy at which a set of IMFP data is consistent with theory (Eq. [1]) and optical data.

Our previous IMFP calculations for 200-2000 eV electrons were analyzed using Fano plots (4). We found linear plots but the slopes were greater than expected from optical data; that is, the electron energies were not high enough to be in the asymptotic Bethe region (11,16). Nevertheless, the Bethe equation did fit the calculated IMFPs empirically over the 200-2000 eV range and we were able to derive parametric expressions for β and γ, with guidance from theory, so that IMFPs could be calculated for other materials (4). This general formula will be referred to later as TPP-1.

Figures 3 and 4 show Fano plots for two prototypical elements, aluminum and gold, which are free-electron-like and non-free-electron-like, respectively. We have modified the Bethe equation by adding two terms in order to fit our IMFPs over the 50-2000 eV range:

$$\lambda = E/\{E_p^2[\beta \ell n(\gamma E) - C/E + D/E^2]\} \quad \text{Å} \qquad [2]$$

Both Inokuti (14) and Ashley (17) have used similar modifications. The solid lines in Figs. 3 and 4 show satisfactory fits to the IMFP data with Eq. [2]. The dashed lines in Figs. 3 and 4 show the first term of Eq. [2] (i.e., the Bethe equation) and the necessity for the other terms.

Similar fits to those of Figs. 3 and 4 have been made using Eq. [2] and the IMFP results for the other 29 materials. We have found empirically that the parameters β, γ, C, and D in Eq. [2] can be represented approximately by the following equations:

$$\beta = -0.0216 + 0.944/(E_p^2 + E_g^2)^{1/2} + 7.39 \times 10^{-4}\rho \qquad [3]$$

$$\gamma = 0.191\rho^{-0.50} \qquad [4]$$

$$C = 0.0650/U^2 - 0.130/U + 1.11 \qquad [5]$$

$$D = 1.91/U^2 - 5.12/U + 35.3 \qquad [6]$$

where E_g is the bandgap energy (in eV) for nonconductors and $U = N_v\rho/A$. Equations [3] and [4] are similar to the corresponding expressions for β and γ derived earlier in fits to the IMFP data over the 200-2000 eV range (TPP-1).

Equations [2] - [6] constitute a new general formula for IMFPs over the 50-2000 eV range and will be referred to as TPP-2. Figures 5 and 6 show plots of the calculated IMFP values for aluminum and gold, fits to these data with Eq. [2], and IMFP values predicted by TPP-2 (using appropriate values of the parameters for each material). It can be seen that TPP-2 provides a reasonable representation of the calculated IMFPs, particularly the very different IMFP-energy dependences for these two elements. In this respect, TPP-2 is superior

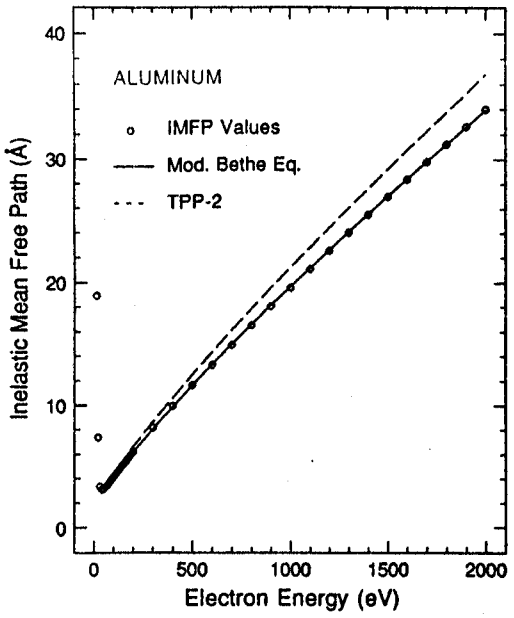

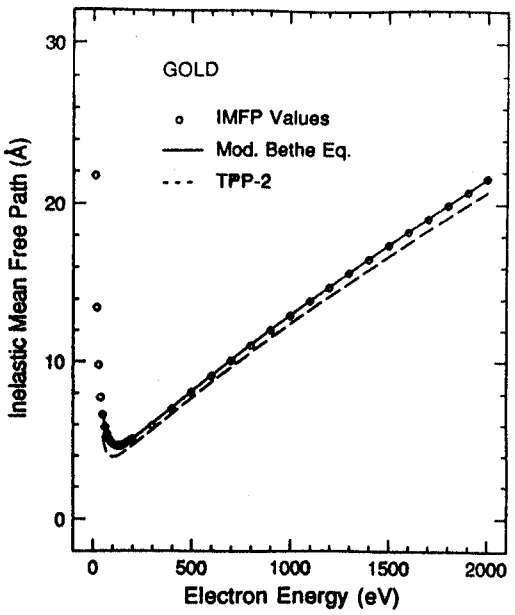

Fig. 5. Comparison of calculated IMFP values for aluminum (open circles) with the fit (solid line) using the modified Bethe equation [Eq. (2)], and the predictions (dashed line) of the general formula TPP-2 [Eqs. (2)-(6)] using values of parameters for Al.

Fig. 6. Comparison of calculated IMFP values for gold (open circles) with the modified Bethe equation (solid line) and the general formula TPP-2 (dashed line) using values of parameters for Au. See caption to Fig. 5.

to the AL formula of Seah and Dench (5). The additional terms in TPP-2 compared to TPP-1 are needed to represent adequately the IMFP dependence on energy for $E \leq 200$ eV, as indicated by Figs. 3 and 4.

The rms errors in the IMFP values calculated by TPP-2 compared to the IMFP values calculated from the Penn algorithm range from 24% at 50 eV to 15% at 100 eV and 14% at 2000 eV. The largest relative errors were around 50% for 50 eV electrons in C, Ni, Cu, and SiO_2. These errors are considered reasonable considering the empirical nature of TPP-2 and the fact that such formulas cannot adequately represent the variations in the electron energy-loss functions for different materials. Nevertheless, TPP-2 is considered to be a useful guide for predicting IMFPs in other materials.

SUMMARY

We have calculated IMFP values over the 50-2000 eV energy range in 31 materials. There are substantial differences in the shapes of the IMFP versus energy curves in the 50-200 eV range. These differences could be understood in terms of variations in the shapes of the electron energy-loss functions.

We found that the IMFP values could be fitted by a modified form of the Bethe equation and that the four parameters in this modified equation could be empirically related to several material constants. The resulting general formula can be used to predict IMFP values in other materials (over the same range of electron energies). Further work is necessary to check the validity of the new formula for other materials. Nevertheless, we believe that the new formula will be useful for predicting the IMFP dependence on energy for a given material (particularly in the lower energy part of the range) and the material-dependence for a given energy.

REFERENCES

1 C.J. Powell, J. Electron Spectrosc. Relat. Phenom., 47 (1988) 197.
2 A. Jablonski and H. Ebel, Surf. Interface Anal., 11 (1988) 627.
3 A. Jablonski, Surf. Science, 188 (1987) 164; A. Jablonski, B. Lesiak, H. Ebel, and M.F. Ebel, Surf. Interface Anal., 12 (1988) 87; H. Ebel, M.F. Ebel, P. Baldauf, and A. Jablonski, Surf Interface Anal., 12 (1988) 172.
4 S. Tanuma, C.J. Powell, and D.R. Penn, Surf. Interface Anal., 11 (1988) 577.
5 M.P. Seah and W.A. Dench, Surf. Interface Anal., 1 (1979) 2.
6 D.R. Penn, Phys. Rev B, 35 (1987) 482.
7 C.J. Powell and M.P. Seah (to be published).
8 V.L. Moruzzi, J.F. Janak, and A.R. Williams, Calculated Electronic Properties of Metals, Pergamon, New York, 1978; D.A. Papaconstantopoulous, Handbook of the Band Structure of Elemental Solids, Plenum, New York, 1986.
9 S. Tanuma, C.J. Powell, and D.R. Penn (to be published).
10 C.J. Powell, in: D.F. Kyser, H. Niedrig, D.E. Newbury, and R. Shimizu (Eds), Electron Beam Interactions with Solids for Microscopy, Microanalysis and Microlithography, Scanning Electron Microscopy, AMF O'Hare, 1984, pp. 19-31.
11 C.J. Powell, Ultramicroscopy, 28 (1989) 24.
12 H. Bethe, Ann. der Physik, 5 (1930) 325.
13 C.J. Powell, Surf. Interface Anal., 7 (1985) 256; ibid. 10 (1987) 349.
14 M. Inokuti, Rev. Mod. Phys., 43 (1971) 297.
15 U. Fano, Phys. Rev., 95 (1954) 1198.
16 F.J. de Heer and M. Inokuti, in: T.D. Märk and G.H. Dunn (Eds), Electron Impact Ionization, Springer, New York, 1985, p. 232.
17 J.C. Ashley, J. Electron Spectrosc. Relat. Phenom., 46 (1988) 199.